





Buckling characteristics of nano-silica doped carbon fiber reinforced composites having cutouts

Hüseyin Özdemir¹  | Özkan Özbek²  | Ömer Yavuz Bozkurt³  |
Ahmet Erklig³ 

¹Faculty of Fine Arts, Textile and Fashion Design Department, Gaziantep University, Gaziantep, Turkey

²Faculty of Engineering, Department of Mechanical Engineering, Pamukkale University, Denizli, Turkey

³Faculty of Engineering, Department of Mechanical Engineering, Gaziantep University, Gaziantep, Turkey

Correspondence

Özkan Özbek, Faculty of Engineering, Department of Mechanical Engineering, Pamukkale University, Denizli 20160, Turkey.

Email: ozbek@pau.edu.tr

Abstract

The current study presents an experimental investigation devoted to the nano-silica and cutout effects on the axial and lateral buckling responses of carbon/epoxy fiber-reinforced composite laminates. To this end, specimens manufactured by vacuum bagging after hand layup technique were prepared at various amounts of nano-silica (0.5%, 1.0%, 1.5%, 2.0%, and 3.0% by weight) incorporated into epoxy resin. Furthermore, semi-circular and circular cutouts were opened on specimens to understand cutout effect on buckling characteristics of specimens. The results demonstrated that nano-silica had a significant effect on buckling behaviors of the carbon fiber-reinforced composites. Regardless of cutout presences, maximum critical axial (393.33 N, 361.67 N, 320 N for W, C and S) and lateral buckling loads (34.67 N, 33 N, 32.33 N for W, C and S), were achieved from the samples having 1.5 wt. % nano-silica. In specimens having no cutout, maximum improvements of 72.26% in axial and 48.6% in lateral directions were achieved from the specimens having 1.5 wt. % nano-silica content. A further amount of nano-silica addition decreased the resistance to buckling of the specimens. Also, the presence of cutouts on the specimens led to decreases in critical loads. The decreases of 1.5 wt. % nano-silica doped specimens without cutout in the axial and lateral critical buckling loads, respectively, were seen as 22.9% and 7.24% for circular cutout, 8.75% and 5.06% for semi-circular cutout. It was concluded that cutout processing and nano-silica additions should be taken into consideration in a material that may be exposed the buckling failures.

Highlights

- Nano-silica impact on buckling behaviors of carbon fiber-reinforced composites
- Cutout effects on buckling properties of carbon fiber-reinforced composites
- Failure modes of carbon fiber-reinforced composites with nano-silica particles
- Findings showed that 1.5 wt. % nano-silica inclusion exhibited the best values for buckling.

This is an open access article under the terms of the [Creative Commons Attribution-NonCommercial](https://creativecommons.org/licenses/by-nc/4.0/) License, which permits use, distribution and reproduction in any medium, provided the original work is properly cited and is not used for commercial purposes.

© 2024 The Authors. *Polymer Composites* published by Wiley Periodicals LLC on behalf of Society of Plastics Engineers.

KEYWORDS

buckling, carbon fiber, cutout, nano-silica

1 | INTRODUCTION

The material selection is the foundation of all engineering applications and design. It influences the product performance goals like reliability, service life, and cost. Various kinds of materials such as metal alloys, ceramics, polymers, and composites are used in a variety of industrial sectors to meet product performance requirements. The selection of materials has many criteria which include strength, stiffness, damping, impact damage resistance, hardness, thermal stability, flammability, weight, fabrication, cost, resistance to corrosion and chemicals. Over the last few decades, impressive progress in the world of engineering materials has occurred and fiber-reinforced composite materials have gained considerable popularity as engineering materials due to their outstanding mechanical properties, in particular high strength and stiffness with low weight, resistance to corrosion, dimensional stability and good damping.¹⁻⁵

Fiber-reinforced composite materials have been widely used in aerospace, marine, and civil engineering applications in the form of relatively thin-walled laminated configurations such as beam, plate, or shell structures.⁶⁻⁹ The composite materials in such applications are subjected to various combinations of in-plane, out-of-plane, and shear loads, and as a result, the buckling phenomenon is often observed. It is a well-known phenomenon that, due to thin sectional structure, composite materials are vulnerable to buckling under compression loads. Because of the large deformation generation at lower stress levels, buckling is one of the critically dangerous failure mechanisms to structural components. This led to a focus on the study of buckling behavior in composite materials. In the literature, many studies regarding the buckling performance of the composite materials are seen.¹⁰⁻¹² Doğan¹³ investigated the graphene nanoplatelets (GNPs) effects on the carbon/aramid fiber-reinforced composite laminates subjected to different boundary conditions. It was reported that GNP addition enhanced the critical loads in both axial and lateral directions. Ferreira et al.¹⁴ performed a numerical study devoted to buckling and post-buckling behaviors of cellular composite beams. Six geometric crosssections were considered as parameters and 120 models were processed. They stated that an increase in web slenderness led to a change in the buckling mode of the structures.

The diversity of shapes, loadings, and edge conditions in engineering applications has engendered a great variety in researches for the buckling behavior of laminated fiber-reinforced composite materials. For this reason, in the literature, a considerable amount of research has been devoted to analytical, numerical, and experimental studies of buckling behavior of laminated fiber-reinforced composite materials. As far as buckling characteristics of laminated fiber-reinforced composite materials are concerned, most of the available literature data refer to plates with and without cutouts.^{15,16} The buckling behavior of rectangular,¹⁷ circular,¹⁸ elliptical,¹⁹ and skew²⁰ plates with different end conditions,²¹⁻²³ loadings,²⁴ number of layers,^{25,26} ply orientations,^{27,28} stacking sequences,^{29,30} aspect ratios,³¹ thicknesses,³² cutout shapes^{33,34} and material nonlinearity³⁵ have been studied by many researchers. However, some techniques that can increase the buckling performance of fiber-reinforced composite materials are also widely preferred. Some of these methods include the use of high-modulus fibers, the addition of micro or nano particles, increasing the number of layers of the composite structure, and the texture architecture used in the composite material. These methods not only increase the overall mechanical performance but also contribute positively to the buckling behavior.³⁶⁻⁴⁰ Amongst these techniques, the incorporation of nano- or micro-sized particles into the resin has great attention in the scientific field due to its direct impact on the mechanical performance of the matrix which is a weaker component of a composite. Several studies devoted to the effect of nanoparticles on the mechanical characteristics of fiber-reinforced composites are seen in the literature.⁴¹⁻⁴⁵ Purahit et al.⁴⁶ investigated the influences of steel industry waste Linz-Donawitz (LD) sludge on the physical, mechanical, and erosion wear properties of the polypropylene-LD sludge composites. While the samples with 20 wt. % filler increased the compressive strength and hardness behaviors, tensile and flexural strength values were dramatically decreased. Özbek et al.⁴⁷ examined the nanoclay impact on the buckling performance of carbon/Kevlar intraply hybrid fiber-reinforced composite laminates. They stated that the specimens having 1 wt. % nanoclay content showed the maximum axial and lateral buckling responses as 21.12% and 25.33% higher compared to specimens without nanoparticles. The excessive inclusion of nanoclay resulted in dramatic decreases of critical buckling loads. Bulut⁴⁸ researched the nanographene

effect on the tensile, flexural, and low-velocity impact properties of basalt fiber-reinforced composite laminates. It was reported that 0.1 wt. % content of nanographene significantly enhanced the mechanical performance of the specimens due to increases in bonding strength in nanoparticle-epoxy-fiber interphases.

Despite its importance in structural applications, there are relatively few studies on buckling properties of nanocomposites in the open literature, and a detailed investigation on how nanoparticles and cutout affect the mechanical stability of the fiber reinforced polymer matrix composites is not available. In this study, the effect of nano-silica and cutout on the axial and lateral buckling behavior of carbon/epoxy composite laminates was investigated. In this context, laminates with different nano-silica contents were produced by vacuum bagging after the hand layup method. The number of layers used was 12 and the carbon fabric in each layer has a 0/90 degree orientation. In addition, configurations without holes, with 2-sided semi-circular holes in the center and with 1 circular hole in the center were also examined. Nano-silica due to its favorable properties such as good adhesion, easy availability, strength, and low cost was

preferred and incorporated into epoxy resin at five different weight percentages (0.5%, 1.0%, 1.5%, 2.0%, and 3.0%).

2 | MATERIALS AND METHODS

2.1 | Specimen preparation

Carbon fabrics having 204 g/cm² areal density were used as reinforcement material in laminates. Epoxy resin (EPIKOTE MGS L160) with 1.18–1.20 g/cm³ density and hardener (EPIKURE Curing Agent MGS H260S) were stirred to obtain a matrix system in a weight ratio of 100:36, respectively. These raw materials were procured from Dost Kimya A.Ş., Turkey. The mechanical properties of the raw materials are given in Table 1.

As a filler material, nano-silica particles having 15 nm average particle size and 99.5% purity were provided from Grafen Chemical Industries Co., Turkey. In order to prepare of matrix phase of the composite laminates, epoxy resin and nano-silica particles were mixed at 8000 rpm for 15 min. Then, the mixture added hardener was mechanically stirred for around 10 min. Five

TABLE 1 Mechanical properties of the raw materials.^{49,50}

Raw material	Tensile strength (MPa)	Tensile modulus (GPa)	Thickness (mm)
Carbon fabric	2500–3000	200–700	0.25
Epoxy (Neat)	70–80	3.2–3.5	-

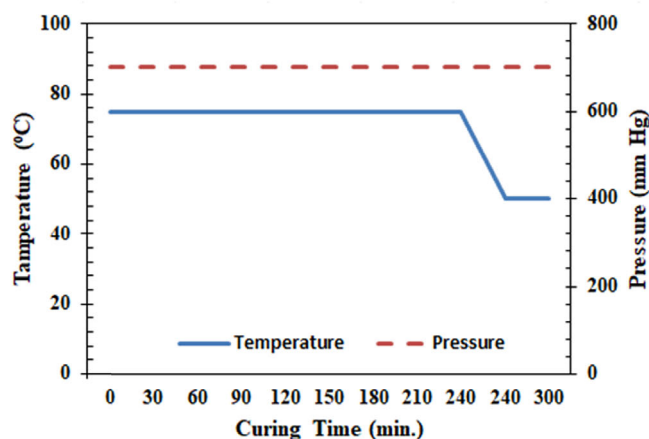
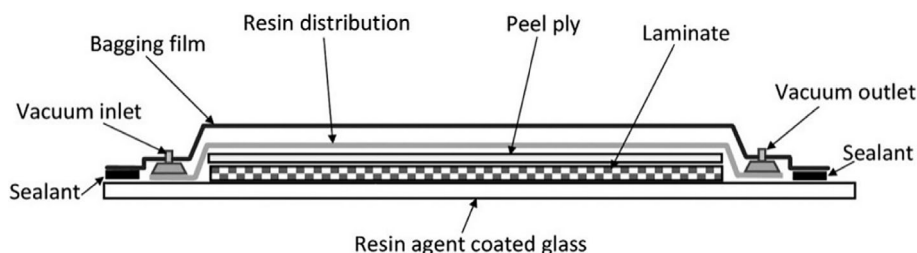


FIGURE 1 (A) Vacuum bagging molding.⁵¹ (B) Curing cycle.

different percentages of nano-silica (0.5%, 1.0%, 1.5%, 2.0%, and 3.0% by weight) were incorporated into epoxy resin.

The process of hand lay-up lamination and vacuum bag molding was carried out to fabricate composite specimens as shown in Figure 1A. A flat rigid aluminum platform equipped with electrical heating elements was coated with a thin layer of mold release agent and used as the bottom mold for the vacuum bagging process. The plain weave aramid fabric was cut into 12 square sheets with a side length of 50 cm using an electric cutter. A small amount of resin mixture layer was applied over the mold and the first fabric layer was placed on it. An appropriate amount of resin mixture was poured down the center of the layer and spread out using a smooth brush to soak into the fabric. The second layer was kept on the first layer and again a resin mixture was poured and spread. The process is repeated for all twelve layers of the stack. Entrapped air bubbles between the layers were removed out of the laminate by the roller. A perforated plastic film and a breather ply were placed on top of the stack and the whole structure was sealed with a vacuum bag. The air was evacuated from the bag with a vacuum pressure of 700 mm Hg to consolidate the layers during the curing process. The curing process was performed at 75°C for 4 h and post curing was carried out at 50°C for 1 h (Figure 1B).

After the fabrication of composite laminates, specimens in dimensions of 200 mm × 20 mm were handled on a CNC router. Also, circular cutouts (3 mm radii) in the middle and semicircular cutouts (3 mm radii) in 2-sided were opened. The dimensions and cutout locations are seen in Figure 2. The thicknesses of the laminates were measured as 2.26 ± 0.2 mm. To ensure experimental reliability, five number of specimens were tested for each configuration. The naming and nano-silica content of the samples are seen in Table 2. W, C, and S represent the without, circular, and semi-circular cutouts, respectively, and the adjacent numbers show the nano-silica percentages in specimens.

2.2 | Buckling experiments

Axial and lateral buckling tests were conducted on a Shimadzu AG-X series electromechanical universal testing machine with a 300 kN load capacity. In the axial buckling test, the test specimen was firstly placed into the upper and lower heads of the machine by aligning the axes of the heads and fixing 20 mm length portions from each side of the specimen with the jaws of the machine heads. It was then compressed by a downward movement of the upper crosshead at a constant speed of 1.0 mm/min. In the lateral buckling test, one end of the test specimen was built into a rigid fixture to eliminate transverse motions and rotations, and the other end (free end) was subjected to loading by the downward displacement of the upper crosshead with a constant speed of 0.25 mm/min. In order to minimize the friction in the contact region of the crosshead and specimen, a ball bearing was installed to free end of the specimen. With the help of interface software installed on the computer connected to the testing machine, the load–displacement curve was plotted with the load and displacement data acquired from the machine and the software automatically stopped testing when the load began to drop. According to the Southwell plot method,⁵² the endpoint of linearity on the initial section of the load–displacement curve was used to

TABLE 2 The naming and nano-silica content of the specimens.

Nano-silica content (wt. %)	Naming (W: without, C: circular, S: semi-circular cutout)
0.0	W, C, S
0.5	W0.5, C0.5, S0.5
1.0	W1, C1, S1
1.5	W1.5, C1.5, S1.5
2.0	W2, C2, S2
3.0	W3, C3, S3

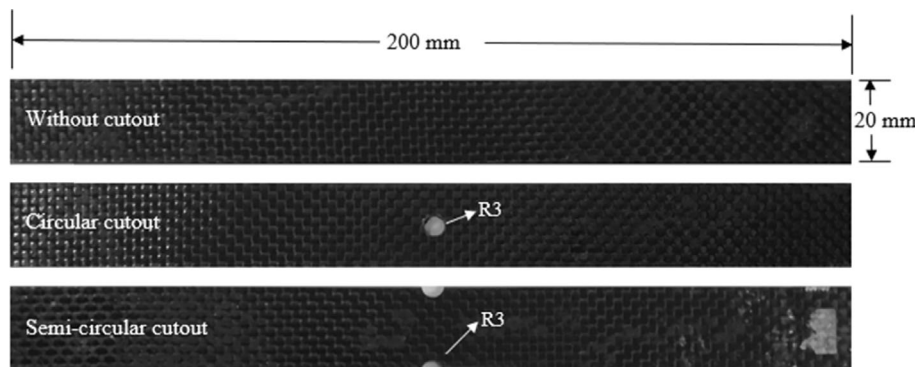


FIGURE 2 Specimen dimensions and cutout locations.

determine the critical buckling load. In an axial or lateral buckling test, the average and standard deviation of values obtained from the test results of five samples for each composite configuration was reported as the critical buckling load. Photos of the experimental setups taken during axial and lateral buckling of the test specimens are presented in Figure 3A,B, respectively.

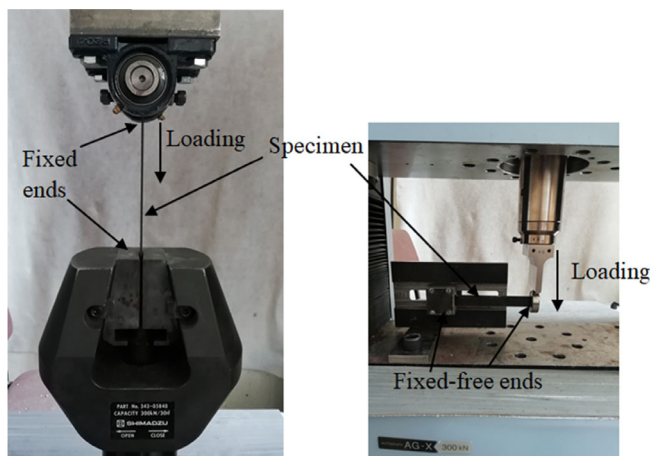


FIGURE 3 Buckling tests; (A) axial buckling, (B) lateral buckling.

3 | RESULTS AND DISCUSSIONS

3.1 | Axial buckling tests

The displacement diagrams of the specimens without and with nano-silica added against axial compressive load for circular, semi-circular, and without cutouts are given in Figure 4. In the graphs, it was seen that there is a linear increase up to a point and continues with a non-linear curve due to the appearance of distortions with the increase in load. Further, load values followed as a linear horizontal line for all configurations. All nano-silica doped specimens showed a better response to axial compressive loading. According to the graphs, pure specimens with circular and semi-circular cut-outs exhibited the earliest buckling failures. The highest load-carrying capacities were obtained from the specimens with 1.5 wt. % nano-silica content. However, as the nano-silica content increased after 1.5 wt. %, the resistance to the buckling load of specimens began to decrease. This can be attributed to an excessive amount of nanoparticle inclusion that resulted in non-uniform distribution. In literature, a lot of studies devoted to nanoparticles have negative effects after a certain amount are seen in the literature.^{47,48}

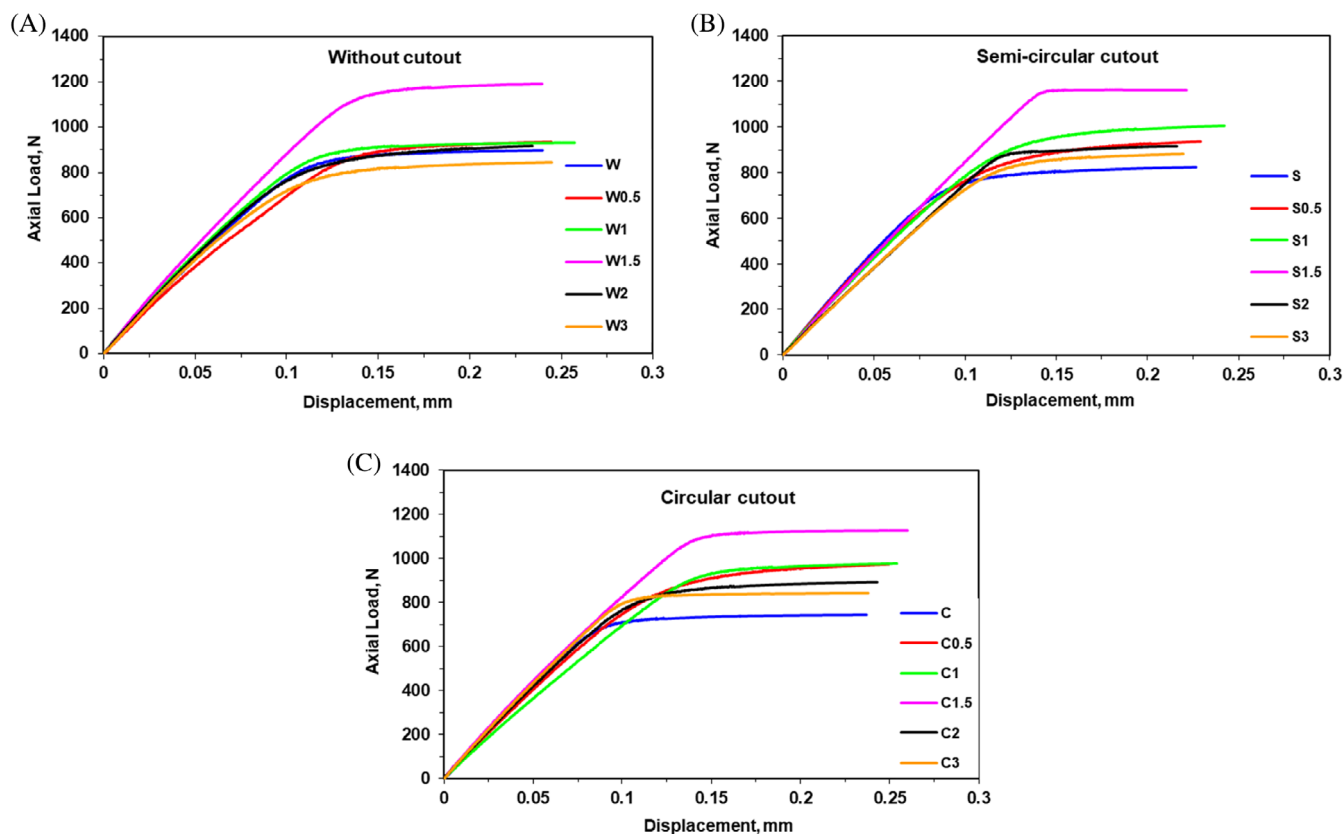


FIGURE 4 Axial load-displacement responses; (A) without cutout, (B) semi-circular cutout, (C) circular cutout.

Specimen	Nano-silica content (wt. %)					
	0.0	0.5	1.0	1.5	2.0	3.0
W	228.33	273.33	326.67	393.33	275.00	253.33
S	222.50	270.00	292.50	361.67	263.75	225.00
C	196.67	265.00	290.00	320.00	253.33	230.00

TABLE 3 Critical buckling loads of carbon/epoxy structures in the axial direction according to nano-silica amounts.

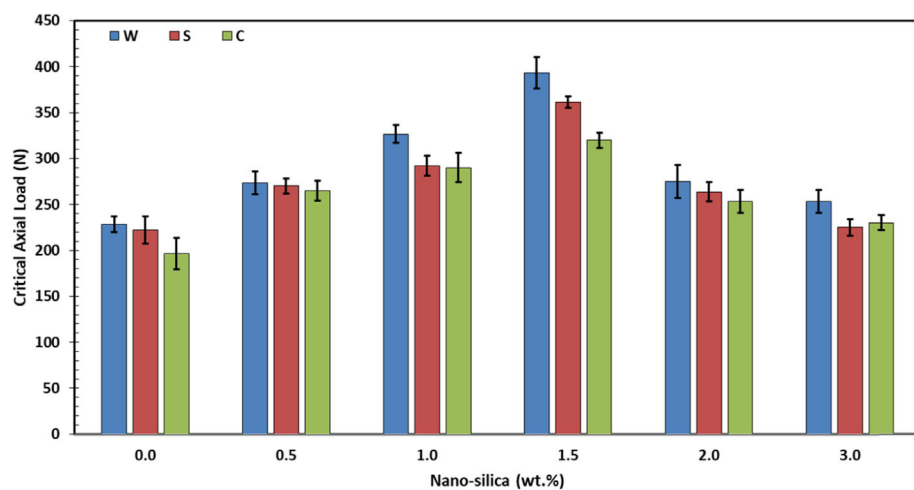


FIGURE 5 Critical axial buckling loads.

The critical axial buckling loads of the specimens are given in Table 3 and Figure 5. The results showed that the maximum critical axial buckling load values were obtained from the specimens with 1.5 wt. % nano-silica. The improvements in without, circular, and semicircular cutout specimens having 1.5 wt. % nano-silica were seen as 72.26%, 62.71%, and 62.55% when compared to pure specimens. Regardless of cutout processing, all nano-silica doped specimens showed a better response against compressive loads. However, more amount of nano-silica addition (higher than 1.5 wt. %) resulted in a decreasing trend in critical axial loads. This can be attributed to the missing homogeneity in the material due to excessive nano-silica might cause some agglomerations or exfoliations leading to local stress concentrations. There are a lot of studies regarding material degradation due to excessive nanoparticle inclusion in the literature.^{53,54} Also, bending formations at the middle region of the specimens were seen as the main causes of the failures due to the compressive loads in axial directions. Additionally, the cutouts leading to a decrease in the stiffness of the specimens exhibited negative effects on the buckling resistance of the specimens. The decreases in the specimen with 1.5 wt. % nano-silica and without cutout were seen as 22.9% and 8.75% for the specimens having circular and semicircular cutouts, respectively. Özbek and Tokur Bozkurt⁵⁵ reported that cutouts had a negative impact on the vibration characteristics of the basalt/carbon hybrid composites due to the reductions in stiffness.

3.2 | Lateral buckling tests

The lateral load and displacement plots of nano-silica doped carbon/epoxy composite specimens are shown in Figure 6. It was observed that all specimens followed a linear path up to the critical point, the specimens showed stable behavior as long as the magnitude of the load on the specimens remained below the critical point. Then, slight deflections and bending of the specimens were observed. Considering the effect of the amount of nano-silica on the lateral load-carrying capacity of the specimens, it can be said that the maximum contribution was obtained from the specimens with 1.5 wt. % nano-silica. However, a higher amount of nano-silica addition decreased the load-carrying capacity of the specimens. This may be attributed to the degradation of the specimens as a result of excessive nanoparticle additions.^{13,48} Also, it can be stated that cutouts, whether circular or semi-circular, exhibited lower resistance to lateral loads due to the stiffness reduction in specimens.

The critical lateral buckling loads of the nano-silica doped specimens according to different cutouts are given in Table 4 and Figure 7. The maximum critical load of 34.67 N was achieved from the 1.5 wt. % nano-silica doped specimen without a cutout, while minimum one (19.67 N) was obtained from the pure specimens with semi-circular cutouts. It was clearly seen that the addition of nano-silica showed significant increases compared to the specimens without nano-silica. The specimens with 1.5% nano-silica were 48.6% higher in pure (23.33 N), 5% higher in S1.5

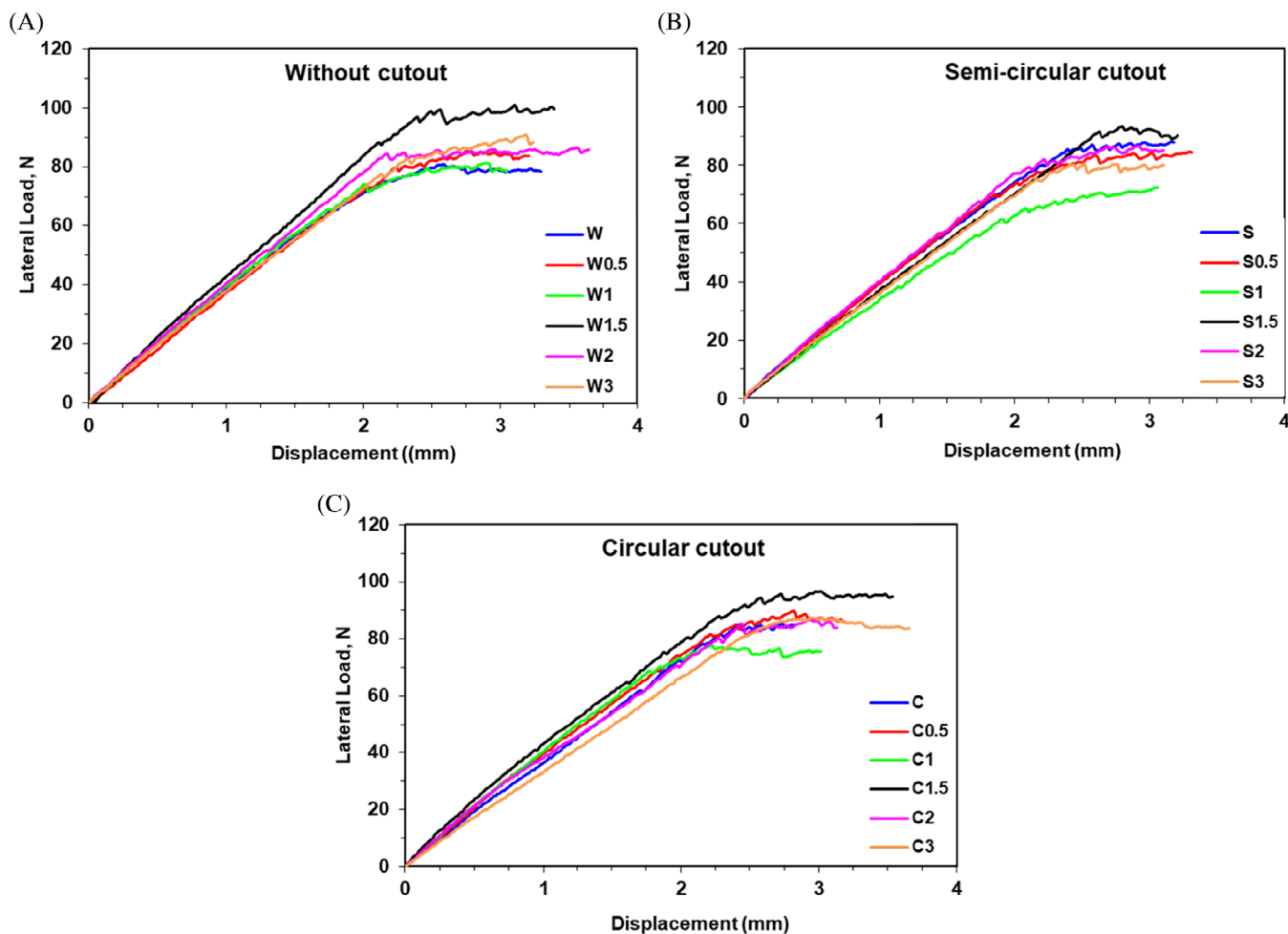


FIGURE 6 Lateral load–displacement responses; (A) without cutout, (B) semi-circular cutout, (C) circular cutout.

TABLE 4 Critical buckling loads of carbon/epoxy structures in the lateral direction according to nano-silica amounts.

Specimen	Nano-silica content (wt. %)					
	0.0	0.5	1.0	1.5	2.0	3.0
W	23.33	29.00	32.67	34.67	32.33	27.00
S	19.67	23.75	28.00	33.00	26.67	25.00
C	23.67	26.33	29.33	32.33	26.33	25.00

(33 N), and 7.24% higher in C1.5. The reason for this increase can be interpreted as the interaction between nano-silica and epoxy matrix can be best achieved at this value. In terms of critical buckling loads in the lateral direction, the values from highest to lowest were obtained from the nano-silica doped specimens of 1.5%, 1%, 2%, 0.5%, 3%, and 0%, respectively. It is possible to say that the high amount of nano-silica resulted in a negative effect due to the degradation of the material. Bozkurt et al.⁵⁴ stated that higher nanoparticle addition can be less

effective in buckling properties of composite laminates due to agglomerations or exfoliations.

Figure 8 represents the behaviors of carbon fiber-reinforced composite specimens under lateral buckling loads. Unlike axial buckling conditions, not only bending but also twisting was seen as the main responsible for lateral buckling failures. Due to the decrease in stiffness of the specimens, the forms of twisting and large displacement in the lateral direction were seen as failure causes.⁵⁶ Also, fiber cracking failures were seen on the clamped side of the samples because it was exposed to higher stress concentrations. Many studies devoted to lateral buckling of the composite laminates stated that a specimen exposed to lateral loads can be buckled due to both bending and twisting.^{47,53}

3.3 | SEM analysis

In this study, the effects of nano-silica particles on damage properties including matrix cracking, debonding,

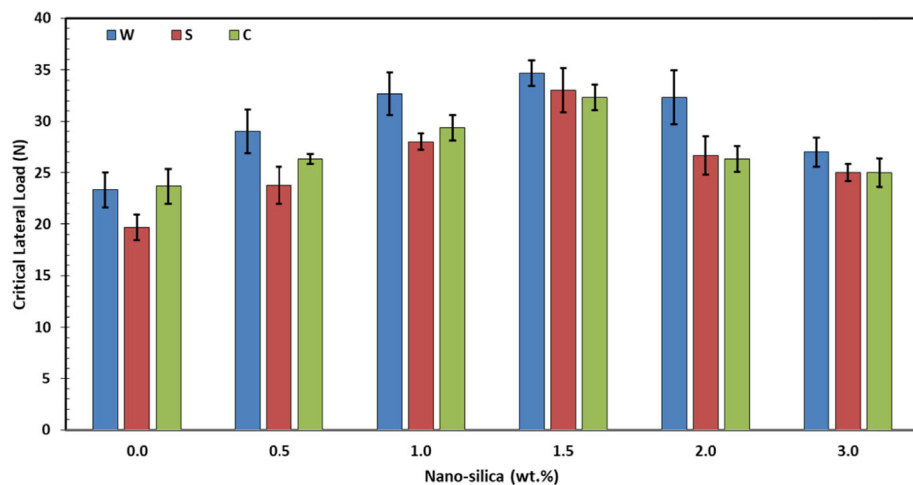


FIGURE 7 Critical lateral buckling loads.



FIGURE 8 Laterally buckled specimen.

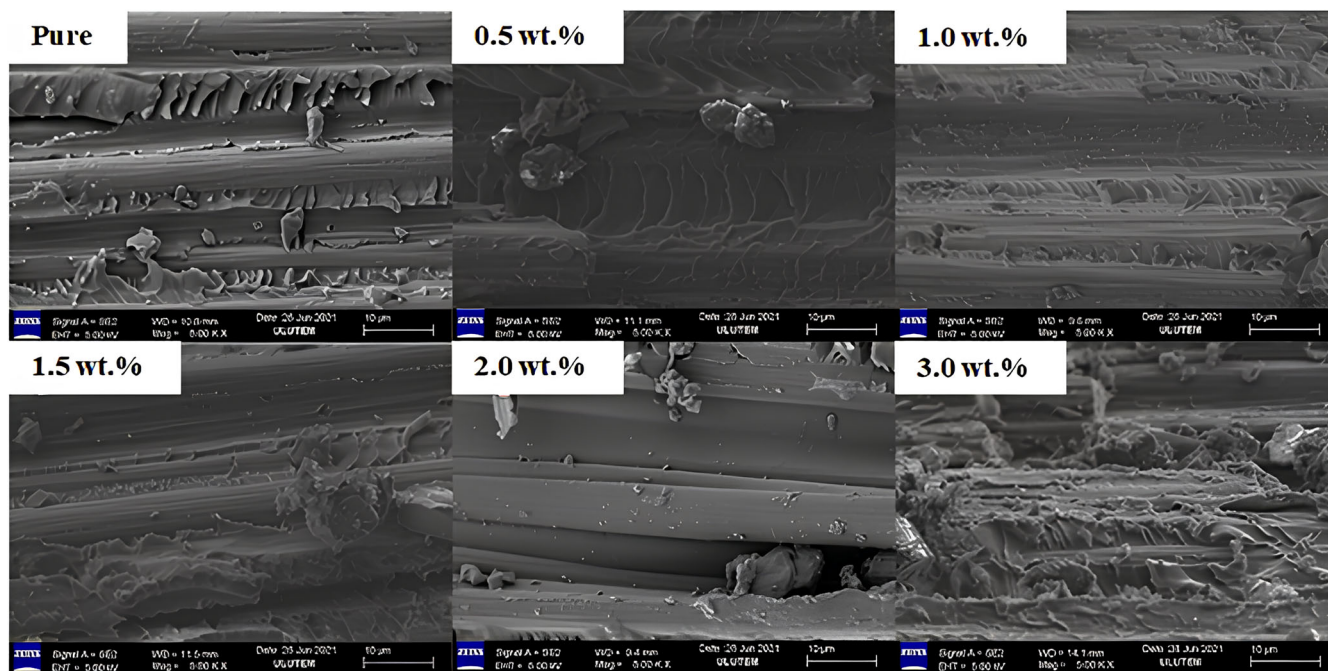


FIGURE 9 SEM micrograph images of specimens.

delamination, and micro-buckling failures were investigated by scanning electron microscopy (SEM) analysis. Figure 9 represents the SEM micrograph images of specimens containing various nano-silica particle percentages. It was seen that pure specimens exhibited high fiber-matrix compatibility and epoxy showed a homogeneous distribution within the structure and formed a good bond with the carbon fiber. This reduced the formation of

delamination in the structures. Also, it was observed that nano-silica addition at various amounts provided positive properties to the structure. However, this contribution varies according to the amount of nano-silica. The best results were obtained in structures with 1.5% nano-silica. At this optimum value, it was observed that the structure formed a good bonding capability, adhesion increased and there was a homogeneous distribution within the

structure. However, the results obtained with the amount of nano silica were not directly proportional. For example, there was a decrease in the mechanical performance of structures with 3% nano-silica. It can be concluded that the increase in the amount of nano silica negatively affects the homogeneity of the structure since some agglomerations and non-homogeneous structures resulted in local stress concentrations and easy degradation of the materials.

4 | CONCLUSIONS


In this study, the effects of cutout and nano-silica on the buckling characteristics of the carbon/epoxy composite laminates were investigated experimentally. Five different nano-silica percentages were incorporated into the epoxy resin and prepared specimens were exposed to axial and lateral compressive loads. According to the results, nano-silica showed that it was a significant filler on the buckling performance of the specimens. Based on the nano-silica effect alone, the maximum critical buckling loads were obtained from samples containing 1.5 wt. % nano-silica. In without cutouts, the specimens with 1.5 wt. % nano-silica exhibited the maximum critical loads of 393.33 N for axial and 34.67 N for lateral. These were 72.26% and 48.6% higher than pure specimens in critical axial and lateral buckling loads, respectively. However, an excessive amount of nano-silica addition such as 2 wt. % or 3 wt. % resulted in a decrease trend. This can be attributed to the formation of agglomerations that cause local stress concentrations. Additionally, cutouts affected the specimens in a negative way due to the decrease in resistance ability to compressive loads.

As a result, the study was a research aimed at improving the buckling properties of the materials used with nanoparticle contribution, taking into account the cutouts that may occur in engineering structures. It has been revealed that cutouts can marginally reduce the strength of materials against buckling loads. On the other hand, nano-silica contribution provided significant increases. In conclusion, the study suggested that nano-silica usage and cutout processing can be considered as a parameter in applications that would be buckling loads.

DATA AVAILABILITY STATEMENT

The data that support the findings of this study are available on request from the corresponding author.

ORCID

Hüseyin Özdemir  <https://orcid.org/0000-0002-0783-0563>

Özkan Özbek  <https://orcid.org/0000-0003-1532-4262>

Ömer Yavuz Bozkurt  <https://orcid.org/0000-0003-0685-8748>

Ahmet Erklığ  <https://orcid.org/0000-0003-3906-3415>

REFERENCES

1. Arslan MH, Yazman Ş, Hamad AA, Aksoylu C, Özkılıç YO, Gemi L. Shear strengthening of reinforced concrete T-beams with anchored and non-anchored CFRP fabrics. *Structure*. 2022;39:527.
2. Oğuz ZA, Erklığ A. Evaluation of the hydrothermal aging effect on the buckling behavior of hybrid glass/aramid/epoxy composite plates: comparison of distilled water and seawater. *Polym Compos*. 2022;43(7):4463-4477.
3. Özkılıç YO, Aksoylu C, Gemi L, Arslan MH. Behavior of CFRP-strengthened RC beams with circular web openings in shear zones: numerical study. *Structure*. 2022;41:1369-1389.
4. Doğan NF, Oğuz ZA, Erklığ A. An experimental study on the hydrothermal aging effect on the free vibration properties of hybrid aramid/glass/epoxy composites: comparison of sea water and distilled water. *Polym Compos*. 2023;44(10):6902-6912.
5. Prabhakar MM, Rajini N, Ayrilmis N, et al. An overview of burst, buckling, durability and corrosion analysis of lightweight FRP composite pipes and their applicability. *Compos Struct*. 2019;230:111419.
6. Gemi L, Köklü U, Yazman Ş. The effects of stacking sequence on drilling machinability of filament wound hybrid composite pipes: Part-1 mechanical characterization and drilling tests. *Compos Part B*. 2020;186:107787.
7. Koconis DB, Kollar LP, Springer GS. Shape control of composite plates and shells with embedded actuators. II. Desired shape specified. *J Compos Mater*. 1994;28(3):262-285.
8. Rikards R, Chate A, Ozolinsh O. Analysis for buckling and vibrations of composite stiffened shells and plates. *Compos Struct*. 2001;51(4):361-370.
9. Oğuz ZA, Özbek Ö, Erklığ A, Bozkurt ÖY. Hydrothermal aging effect on crushing characteristics of intraply hybrid composite pipes. *Eng Struct*. 2023;297:117011.
10. Erklığ A, Yeter E, Bulut M. The effects of cut-outs on lateral buckling behavior of laminated composite beams. *Compos Struct*. 2013;104:54-59.
11. Wodesenbet E, Kidane S, Pang SS. Optimization for buckling loads of grid stiffened composite panels. *Compos Struct*. 2003;60(2):159-169.
12. Ferreira AJM, Barbosa JT. Buckling behaviour of composite shells. *Compos Struct*. 2000;50(1):93-98.
13. Doğan NF. Buckling analysis of graphene nanoplatelets-doped carbon/aramid hybrid polymer composite plates. *Polym Compos*. 2021;42(11):5712-5720.
14. Ferreira FPV, Tsavdaridis KD, Martins CH, De Nardin S. Buckling and post-buckling analyses of composite cellular beams. *Compos Struct*. 2021;262:113616.
15. Wyslowski P, Falkowicz K, Filipek P. Buckling state analysis of compressed composite plates with cut-out. *Compos Struct*. 2021;274:114345.
16. Erklığ A, Yeter E. The effects of cutouts on buckling behavior of composite plates. *Sci Eng Compos Mater*. 2012;19(3):323-330.
17. Mehrabadi SJ, Aragh BS, Khoshkhashesh V, Taherpour A. Mechanical buckling of nanocomposite rectangular plate

- reinforced by aligned and straight single-walled carbon nanotubes. *Compos Part B*. 2012;43(4):2031-2040.
18. Maghamikia S, Jam JE. Buckling analysis of circular and annular composite plates reinforced with carbon nanotubes using FEM. *J Mech Sci Technol*. 2011;25(11):2805-2810.
 19. Ghaheri A, Keshmiri A, Taheri-Behrooz F. Buckling and vibration of symmetrically laminated composite elliptical plates on an elastic foundation subjected to uniform in-plane force. *J Eng Mech*. 2014;140(7):04014049.
 20. Mishra BB, Kumar A, Samui P, Roshni T. Buckling of laminated composite skew plate using FEM and machine learning methods. *Eng Comput*. 2021;38(1):501-528.
 21. Kumar D, Singh SB. Effects of boundary conditions on buckling and postbuckling responses of composite laminate with various shaped cutouts. *Compos Struct*. 2010;92(3):769-779.
 22. Al-Hassani STS, Darvizeh M, Haftchenari H. An analytical study of buckling of composite tubes with various boundary conditions. *Compos Struct*. 1997;39(1-2):157-164.
 23. Singh V, Kumar P, Srivastava VK. Influence of cement particles on the mechanical and buckling behavior of laminated GFRP composites with variation of end conditions of buckling. *Mater Res Express*. 2018;5(6):065323.
 24. Meyer-Piening HR, Farshad M, Geier B, Zimmermann R. Buckling loads of CFRP composite cylinders under combined axial and torsion loading – experiments and computations. *Compos Struct*. 2001;53(4):427-435.
 25. Maali M, Bayrak B, Kiliç M, Sagioglu M, Aydin AC. Buckling behavior of double-layered composite cylindrical shells. *Int J Press Vessel Pip*. 2021;191:104328.
 26. Liu X, Featherston CA, Kennedy D. Buckling optimization of blended composite structures using lamination parameters. *Thin-Walled Struct*. 2020;154:106861.
 27. Rajanna T, Banerjee S, Desai YM, Prabhakara DL. Effect of reinforced cutouts and ply-orientations on buckling behavior of composite panels subjected to non-uniform edge loads. *Int J Struct Stab Dyn*. 2018;18(4):1850058.
 28. Mouhat O, Bybi A, El Bouhmidia A, Rougui M. The effects of ply orientation on nonlinear buckling of aircraft composite stiffened panel. *Frat Ed Integrita Strutt*. 2019;13(50):126-140.
 29. Jing Z, Fan X, Sun Q. Stacking sequence optimization of composite laminates for maximum buckling load using permutation search algorithm. *Compos Struct*. 2015;121:225-236.
 30. de Almeida FS. Stacking sequence optimization for maximum buckling load of composite plates using harmony search algorithm. *Compos Struct*. 2016;143:287-299.
 31. Shrivastava AK, Singh RK. Effect of aspect ratio on buckling of composite plates. *Compos Sci Technol*. 1999;59(3):439-445.
 32. Wankhade RL, Niyogi SB. Buckling analysis of symmetric laminated composite plates for various thickness ratios and modes. *Innov Infrastruct Solut*. 2020;5(3):65.
 33. Taheri-Behrooz F, Omidi M, Shokrieh MM. Experimental and numerical investigation of buckling behavior of composite cylinders with cutout. *Thin-Walled Struct*. 2017;116:136-144.
 34. Ghannadpour SAM, Najafi A, Mohammadi B. On the buckling behavior of cross-ply laminated composite plates due to circular/elliptical cutouts. *Compos Struct*. 2006;75(1-4):3-6.
 35. Wang SS, Srinivasan S, Hu HT, HajAli R. Effect of material nonlinearity on buckling and postbuckling of fiber composite laminated plates and cylindrical shells. *Compos Struct*. 1995;33(1):7-15.
 36. Rafiee MA, Rafiee J, Yu ZZ, Koratkar N. Buckling resistant graphene nanocomposites. *Appl Phys Lett*. 2009;95:223103.
 37. Song M, Yang J, Kitipornchai S. Bending and buckling analyses of functionally graded polymer composite plates reinforced with graphene nanoplatelets. *Compos Part B Eng*. 2018;134:106-113.
 38. Pantano A, Parks DM, Boyce MC. Mechanics of deformation of single- and multi-wall carbon nanotubes. *J Mech Phys Solids*. 2004;52:789-821.
 39. Martino L, Guigo N, van Berkel JG, Sbirrazzuoli N. Influence of organically modified montmorillonite and sepiolite clays on the physical properties of bio-based poly(ethylene 2,5-furandicarboxylate). *Compos Part B Eng*. 2017;110:96-105.
 40. Gul U, Aydogdu M. Noncoaxial vibration and buckling analysis of embedded double-walled carbon nanotubes by using doublet mechanics. *Compos Part B Eng*. 2018;137:60-73.
 41. Tokur Bozkurt Y, Bulut M, Erklig A, Ozbek O. SiO₂ nanoparticle modified CFRP composites effecting on mechanical and vibration damping properties. *Polym Compos*. 2024;45(1):169-180.
 42. Mirzapour Roudpishi M, Hosseini Farrash SM, Shaterzadeh A. Effect of zinc oxide nanoparticles on critical buckling load of glass/epoxy composites exposed to sunlight irradiation. *Polym Polym Compos*. 2023;31:09673911231202153.
 43. Purohit A, Pradhan P, Gupta G, Jena H, Singh J. Sliding wear characterization of epoxy composites filled with wood apple dust using Taguchi analysis and finite element method. *J Vinyl Addit Technol*. 2023;1-13, Early view. doi:10.1002/vnl.22085
 44. Jena H, Pradhan P, Purohit A. Dielectric properties, thermal analysis, and conductivity studies of biodegradable and biocompatible polymer nanocomposites. *Biodegradable Biocompatible Polym Nanocompos*. 2023;113-140.
 45. Swain PTR, Das SN, Patnaik PK, Purohit A. The influence of moisture absorption on the mechanical and thermal properties of chemically treated DPL reinforced hybrid composite. *Mater Sci Forum*. 2020;978:316-322.
 46. Purohit A, Gupta G, Pradhan P, Agrawal A. Development and erosion wear analysis of polypropylene/Linz-Donawitz sludge composites. *Polym Compos*. 2023;44(10):6556-6565.
 47. Özbek Ö, Doğan NF, Bozkurt ÖY, Erklig A. Assessment of nanoclay impact on buckling response of carbon/Kevlar hybrid composites. *Polym Compos*. 2023;44(2):1421-1429.
 48. Bulut M. Mechanical characterization of basalt/epoxy composite laminates containing graphene nanopellets. *Compos Part B Eng*. 2017;122:71-78.
 49. Bulut M. *Investigation of Impact Behavior of Laminated Hybrid Composite Plates*, Ph.D. Thesis in Mechanical Engineering, Gaziantep University. 2017.
 50. <https://www.dostkimya.com/Documents/mgs-laminasyon-epoksi-re%C3%A7ine-1160.pdf> Date of visit: 08.02.2024
 51. Bozkurt ÖY, Erklig A, Bulut M. Hybridization effects on charpy impact behavior of basalt/aramid fiber reinforced hybrid composite laminates. *Polym Compos*. 2018;39:467-475.
 52. Southwell RV. On the analysis of experimental observations in problems of elastic stability. *Proc R Soc London SerA*. 1932;135:601.
 53. Özbek Ö. Axial and lateral buckling analysis of kevlar/epoxy fiber-reinforced composite laminates incorporating silica nanoparticles. *Polym Compos*. 2021;42(3):1109-1122.
 54. Bozkurt ÖY, Bulut M, Erklig A, Faydh WA. Axial and lateral buckling analysis of fiber reinforced S-glass/epoxy composites containing nano-clay particles. *Compos Part B Eng*. 2019;158:82-91.

55. Özbek Ö, Bozkurt YT. Effect of cut-outs on the free vibration response of basalt/carbon hybrid composites. *Afyon Kocatepe Üniversitesi Fen Ve Mühendislik Bilimleri Dergisi*. 2021;21(3): 724-734.
56. Zhu R, Li F, Zhang D. Overall buckling behaviour of laminated CFRP tubes with off-axis ply orientation in axial compression. *Sci Eng Compos Mater*. 2019;26(1):230-239.

How to cite this article: Özdemir H, Özbek Ö, Bozkurt ÖY, Erklığ A. Buckling characteristics of nano-silica doped carbon fiber reinforced composites having cutouts. *Polym Compos*. 2024; 1-11. doi:[10.1002/pc.28293](https://doi.org/10.1002/pc.28293)